Radiation Physics and Chemistry 107 (2015) 160–163

Contents lists available at ScienceDirect

Radiation Physics and Chemistry

journal homepage: www.elsevier.com/locate/radphyschem

Resonant Raman scattering background in XRF spectra of binary samples

Héctor Jorge Sánchez *, Juan José Leani

Facultad de Matemática Astronomía y Física, Universidad Nacional de Córdoba, 5000 Córdoba, Argentina; and CONICET, Argentina

HIGHLIGHTS

- Influence of resonant Raman scattering in x-ray fluorescence analysis.
- Theoretical calculations of resonant Raman scattering intensities.
- Improving of minimum detection levels in x-ray spectrometry.

ARTICLE INFO

Article history:
Received 17 October 2013
Received in revised form
22 October 2014
Accepted 25 October 2014
Available online 29 October 2014

Keywords:
X-ray fluorescence analysis
Detection limits
Background
Resonant Raman scattering

ABSTRACT

In x-ray fluorescence analysis, spectra present singular characteristics produced by the different scattering processes. When atoms are irradiated with incident energy lower and close to an absorption edge, scattering peaks appear due to an inelastic process known as resonant Raman scattering. In this work we present theoretical calculations of the resonant Raman scattering contributions to the background of x-ray fluorescence spectra of binary samples of current technological or biological interest. On one hand, a binary alloy of Fe with traces of Mn (Mn: 0.01%, Fe: 99.99%) was studied because of its importance in the stainless steels industries. On the second hand a pure sample of Ti with V traces (Ti: 99%, V: 1%) was analyzed due to the current relevance in medical applications. In order to perform the calculations the Shiraiwa and Fujino's model was used to calculate characteristic intensities and scattering interactions. This model makes certain assumptions and approximations to achieve the calculations, especially in the case of the geometrical conditions and the incident and take-off beams. For the binary sample studied in this work and the considered experimental conditions, the calculations show that the resonant Raman scattering background is significant under the fluorescent peak, affects the symmetry of the peaks and, depending on the concentrations, overcomes the enhancements contributions (secondary fluorescence).

1. Introduction

When atoms are irradiated by x-ray photons different kind of interactions take place: the photon can be absorbed by the photoelectric effect or can suffer a Rayleigh or Compton scattering. However, under resonant conditions, other low probability interactions can occur. One of these interactions is the resonant Raman scattering (RRS) (Karydas and Paradellis, 1997).

The x-ray RRS is an inelastic scattering process which presents fundamental differences compared to other scattering interactions between x rays and atoms; when the energy of the incident photon approaches from below to the absorption edge of the target element, a strong resonant behavior takes place contributing to the attenuation of x rays in matter. According to the absorption–emission model the RRS process can be represented by three steps (Sánchez et al., 2006):

1) The initial state consists of an incident photon with an energy below the K (or L3, L2,…) threshold.
2) A hole is produced in the K (or L3, L2, …) shell and the excited electron is ejected to an unoccupied state; an electron from a higher shell fills the vacancy and a photon is emitted.
3) The final state consists of a hole in a higher shell, a scattered photon and an excited electron (in the continuum or in a bound excited state).

Fig. 1 represents the scattering process when the incident photon has an energy below to the K absorption edge and the K hole is filled by an electron from the L shell. This is the KL-type scattering. The incident photon has an energy E_0 lower than the Ω_K energy of the K threshold; the energy of the incident photon is

* Corresponding author.
E-mail address: jsan@famaf.unc.edu.ar (H.J. Sánchez).

http://dx.doi.org/10.1016/j.radphyschem.2014.10.009
0969-806X/

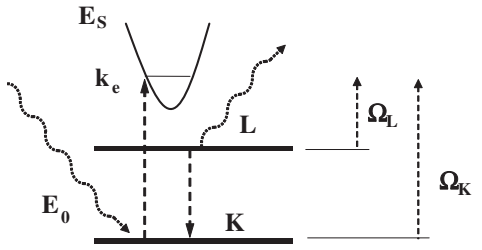

Fig. 1. Schematic representation of a KL resonant Raman scattering process.

absorbed by a K shell electron producing a hole and an electron in the continuum with kinetic energy k_e. The K shell vacancy is filled by an electron from the L shell (being Ω_L the energy of the L threshold) and a scattered photon is emitted with energy E_S.

Assuming a well-defined energy of the incident photon, the energy conservation for the scattering process leads to the following equation (Rubensson, 2000):

$$E_0 - \Omega_L - E_f = E_S + k_e \quad (1)$$

where E_f is the Fermi energy. This equation indicates that between initial and final states the available energy $E_0 - \Omega_L - E_f$ has to be shared between the outgoing electron and the emitted photon.

The resonant character of the process and the existence of an onset energy in the RRS spectrum enable the probing of the edge structure characteristics by tuning the incident energy towards the edge.

The resonant Raman effect was first observed by Sparks in 1974 (Sparks, 1974) and explained theoretically by Bannet and Freund one year later Bannet and Freund (1975). In the last decade, several works have been published showing different measurements related to RRS (Sánchez et al., 2006; Hayashi, 2011; Valentinuzzi et al., 2008; Leani et al., 2011a, 2011b; Hamalainen et al., 1989; Manninen et al., 1985; Suortti et al., 1987), indicating an increasing interest in this phenomenon. As we will see later, this inelastic process can increase the background of the fluorescent line. In specific experimental conditions the RRS must be taken into account when samples constituted by elements with proximate atomic numbers are analyzed because this effect affects the determination of low concentration contaminants. The experimental values of mass attenuation coefficients differ from the theoretical values when materials are analyzed with monochromatic x-ray beams under resonant conditions.

At present, different analytical techniques are used to characterize samples of current interest. Samples are important because of their technological applications or the biological impact of them. In particular, x-ray fluorescence analysis and its variations (total reflection, micro-XRF, etc.) are frequently used to determine concentrations which are critical for the further purpose of the samples. In these cases a correct quantification is imposing and a precise determination of the different atomic processes contributions is of significant relevance.

The aim of this work is to contribute improving the elemental quantification of binary samples by specifying the importance of the RRS in the background of experimental spectra.

2. Calculations and data processing

The basic procedure to calculate fluorescent intensities was presented by Sherman in 1955 (Sherman, 1955) and Shirawa and Fujino in 1966 (Shiraiwa and Fujino, 1966). Corrections to these equations were proposed later by Li-Xing in 1984 (Li–Xing, 1984) and Fernández and Rubio in 1989 (Fernández and Rubio, 1989).

Table 1
Notation.

Symbol	Definition
$H^R(E)$	Normalization factor defined as A in equation (13) of Ref. Sánchez et al., (2006).
R_Z	Concentration of element i multiplied by its fluorescent yield
Ω_{Ki}, Ω_{Li}	Binding energies for the I line of the K and L edge respectively
E_f	Fermi energy
E	Energy of the incident beam
$\tau_i(E)$	Mass photoabsorption coefficient of element i at energy E
$\sigma_j^c(E)$,$\sigma_j^i(E)$	Total coherent (c) and incoherent (i) scattering cross sections for element j at energy E
ω_{ip}	Fluorescence yield of element i, line p
J_{ip}	Absorption edge jump for line p of element i
f_{ip}	Emission probability of line p, element i
C_i	Weight fraction of element i in the sample

In these works, several assumptions, approximations and considerations were made, regarding the geometry of the x-ray beam and sample, physical constants and parameters, etc. The same assumptions will be applied in this work.

Unlike fluorescent processes and coherent scattering, the RRS presents a scattered energy distribution for a given incident energy; therefore the emission factor for resonant Raman interactions is expressed as follows (Bannet and Freund, 1975; Leani et al., 2011):

$$Q_i^r(E, E') = \int_0^{E - \Omega Li + Ef} \frac{H^R(E)\ R_z\ E'}{(\Omega_{Ki} - E)\left[(\Omega_{Ki} - \Omega_{Li} - E')^2 - Ef^2 \right]} dE' \quad (2)$$

The fitting variables are the upper limit of the integral.

The emission factors for fluorescence, coherent and Compton scattering are $Q_{ip}^f(E) = C_i \omega_{ip} J_{ip} f_{ip} \tau_i(E)$, $Q^c(E) = \sum_j C_j \sigma_j^c(E)$ and $Q^i(E) = \sum_j C_j \sigma_j^i(E)$ respectively. Notation regarding the emission factors and Eq. (2) is shown in Table 1.

3. Results and discussions

Calculations were performed using MathCAD 13 (Mathsoft Engineering & Education, Inc.). At the beginning of the code, the parameters of calculations were defined and later the equations were written straightforward as presented in the previous section. Integrations were accomplished by a Newton procedure for numerical integration and not using the internal routine of MathCAD in order to avoid divergences during calculations. In the calculations, mass attenuation coefficients were taken from Hubbell and Seltzer (1995), emission probabilities were obtained from Scofield (1969, 1974) and Khan and Karimi, Khan and Karimi (1980) fluorescence yields were taken from the compilation of Hubbell et al. (1994) and the energies of the emission and absorption lines were those compiled by Bearden (1969), Birks (1974) and Bearden and Burr (1967).

For the calculations binary samples were considered irradiated by a continuum spectrum emitted from an x-ray tube. The analytical description of the x-ray tube intensity, $I(E)$, corresponds to a Mo x-ray tube (Philips PW2275/20) in the 3–45 keV range, which was characterized by the procedure proposed by Mainardi and Barrea (1996), giving the following expression:

$$I(E) = \left(\frac{E_{max}}{E} - 1 \right)^{0.8584} e^{[0.0546\,\mu(4,E) - 0.00525\,\mu(42,E)]} + I_\alpha \delta(E - E_\alpha) + I_\beta \delta(E - E_\beta)$$

where E_{max} is the maximum energy the spectrum, $\mu(Z,E)$ is the mass absorption coefficient of element Z at energy E, I_α and I_β are

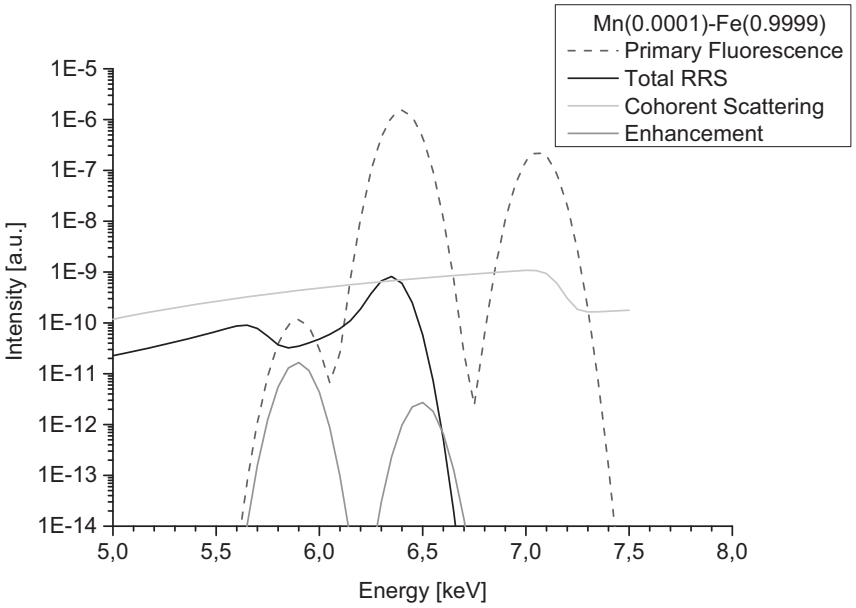

Fig. 2. Mn–Fe sample. Results of calculations for primary florescence (dash), resonant Raman scattering (black), coherent scattering (light gray) and enhancement (gray).

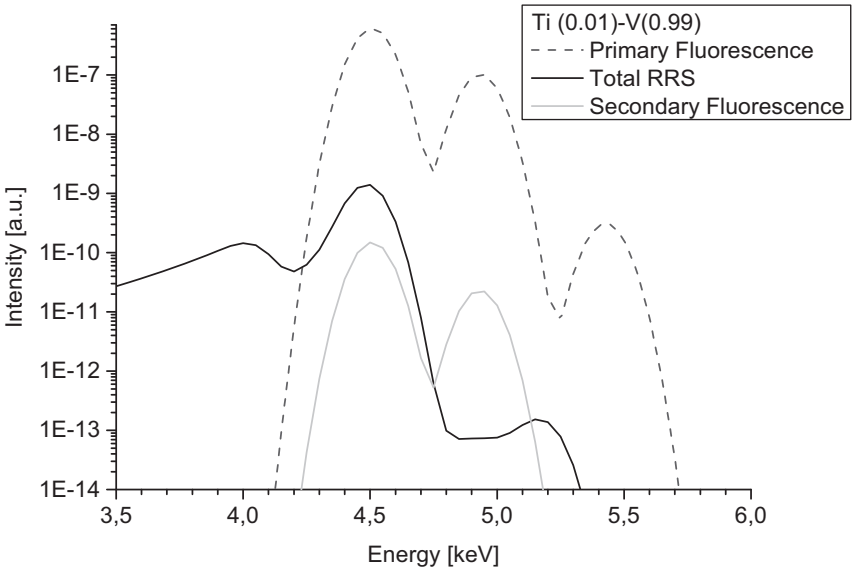

Fig. 3. Ti–V sample. Results of calculations for primary florescence (dash), resonant Raman scattering (black) and secondary fluorescence (light gray).

the intensities of the characteristic lines of the target and E_α and E_β are the energies of the characteristic lines of the target.

Samples were chosen according to the relevance of their applications. On one hand, a binary alloy of Fe with traces of Mn was studied because of its importance in the stainless steels industries. On the second hand a pure sample of Ti with V traces was analyzed due to the current relevance in medical applications. The concentrations under analysis were Mn (0.01%) and Fe (99.99%) and a sample of Ti (99%) contaminated with V (1%). Results are shown in Figs. 2 and 3.

Fig. 2 shows the contributions of coherent scattering in order to compare the different sources of background. As can be seen, the resonant Raman contribution under the Mn peak (5.9 keV) is higher than the coherent background and one order of magnitude higher than the secondary emissions, in addition in the low energy region the contribution of the RRS from Fe turns out to be considerable since it is located under the Mn fluorescent peak, resulting in a final contribution with an asymmetric shape.

The contribution of RRS to the background of the Ti–V alloy is shown in Fig. 3. As can be observed, the resonant Raman contribution from V affects the Ti florescent peak and its contribution must be considered during quantification in order to obtain accurate and reliable results.

4. Conclusions

The results presented in this paper show that the RRS contributes significantly to the background of x-ray fluorescence spectra. These results indicate that resonant Raman contributions have to be considered during quantification in order to obtain precise concentrations. For the considered samples and the

assumed experimental conditions, the calculations carried out in this work show that the RRS background is significant under the fluorescent peak, affects the symmetry of the peaks and, depending on the concentrations, overcomes the enhancements contributions (secondary fluorescence).

The calculation procedure can be implemented prior the experiment in order to predict the effect of RRS and anticipate its contribution.

References

Bannet, Y., Freund, I., 1975. Phys. Rev. Lett. 34, 372.
Bearden, J.A., Burr, A.F., 1967. Rev. Mod. Phys. 39, 125.
Bearden, J.A., 1969. Rev. Mod. Phys. 39, 78.
Birks, L.S., 1974. In: Robinson, J.W. (Ed.), Handbook of Spectroscopy, Vol. I. CRC Press, Cleveland. OH, pp. 1–254.
Fernández, J., Rubio, M., 1989. X Ray Spectrom 18, 281.
Hamalainen, K., Manninen, S., Suortti, P., Collins, S.P., Cooper, M.J., Laundy, D., 1989. J. Phys.: Condens. Matter 1, 5955.
Hayashi, H., 2011. X Ray Spetrom. 40, 24.
Hubbell, J.M., Seltzer, S.M., 1995. Tables of X-Ray Mass Absorption Coefficients and Mass Energy, NISTIR 5632.
Hubbell, H., Trehan, P.N., Singh, N., Chand, B., Mehta, D., Garg, M.L., Garg, R.R., Singh, S., Puri, S., 1994. J. Phys. Chem. Ref. Data 23, 339.
Karydas, A.G., Paradellis, T., 1997. J. Phys. B: At. Mol. Opt. Phys. 30, 1893.
Khan, Md. R., Karimi, M., 1980. X Ray Spectrom 9, 32.
Leani, J.J., Sánchez, H., Valentinuzzi, M.C., Pérez, C., 2011a. J. Anal. At. Spectrom. 26, 378.
Leani, J.J., Sánchez, H., Valentinuzzi, M.C., Pérez, C., 2011b. X-Ray Spectrom. 40, 254.
Li-Xing, Z., 1984. X Ray Spectrom. 13, 52.
Mainardi, R., Barrea, R.A., 1996. X Ray Spectrom 25, 190.
Manninen, S., Alexandropoulos, N.G., Cooper, M.J., 1985. Philos. Mag. B 52, 899.
Mathsoft Engineering & Education, Inc., ⟨www.ptc.com/products/mathcad/⟩.
Rubensson, J., 2000. Electron Spectrosc. Relat. Phenom. 110–111, 135.
Scofield, J.H., 1969. Phys. Rev. 179, 9.
Scofield, J.H., 1974. Phys. Rev. A 9, 1041.
Sherman, J., 1955. Spectrochim. Acta 7, 283.
Shiraiwa, T., Fujino, N., 1966. Jpn. J. Appl. Phys. 5, 886.
Sparks, C.J., 1974. Phys. Rev. Lett. 33, 262.
Suortti, P., Etelaniemi, V., Hamalainen, K., Manninen, S., 1987. J. Phys. Colloq. 48 (C9), 831.
Sánchez, H.J., Valentinuzzi, M.C., Pérez, C., 2006. J. Phys. B: At. Mol. Opt. Phys. 39, 1.
Valentinuzzi, M.C., Sánchez, H.J., Abraham, J., Pérez, C., 2008. X Ray Spectrom. 37, 555.